



Junction analysis and temperature effects in semi-conductor heterojunctions  
by Naresh Tandan

A thesis submitted to the Graduate Faculty in partial fulfillment of the requirements for the degree of  
DOCTOR OF PHILOSOPHY in Electrical Engineering  
Montana State University  
© Copyright by Naresh Tandan (1974)

Abstract:

A new classification for semiconductor heterojunctions has been formulated by considering the different mutual positions of conduction-band and valence-band edges.

To the nine different classes of semiconductor heterojunction thus obtained, effects of different work functions, different effective masses of carriers and types of semiconductors are incorporated in the classification. General expressions for the built-in voltages in thermal equilibrium have been obtained considering only nondegenerate semiconductors. Built-in voltage at the heterojunction is analyzed. The approximate distribution of carriers near the boundary plane of an abrupt n-p heterojunction in equilibrium is plotted. In the case of a p-n heterojunction, considering diffusion of impurities from one semiconductor to the other, a practical model is proposed and analyzed. The effect of temperature on built-in voltage leads to the conclusion that built-in voltage in a heterojunction can change its sign, in some cases twice, with the choice of an appropriate doping level. The total change of energy discontinuities ( $\Delta E_c + \Delta E_v$ ) with increasing temperature has been studied, and it is found that this change depends on an empirical constant and the  $0^\circ\text{K}$  Debye temperature of the two semiconductors. The total change of energy discontinuity can increase or decrease with the temperature. Intrinsic semiconductor-heterojunction devices are studied? band gaps of value less than 0.7 eV. are suggested if such devices are to be used at room temperature. Built-in voltage in the case of intrinsic semiconductor heterojunction devices varies slightly with the temperature. With -proper choice of effective masses, the built-in voltage remains essentially constant with the temperature. The advantages of intrinsic semiconductor devices are discussed. A three-dimensional energy-distance-momentum diagram is described; it suggests a change in the wave vector of a carrier, in transit from one semiconductor to other. Thus, the probability of transition of a carrier across the heterojunction is reduced.

JUNCTION ANALYSIS AND TEMPERATURE EFFECTS  
IN SEMICONDUCTOR HETEROJUNCTIONS

by

NARESH TANDAN

A thesis submitted to the Graduate Faculty in partial  
fulfillment of the requirements for the degree

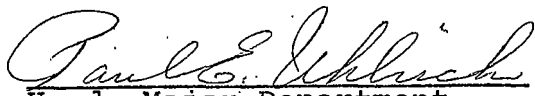
of

DOCTOR OF PHILOSOPHY

in

Electrical Engineering

Approved:

  
Head, Major Department

  
Chairman, Examining Committee

  
Graduate Dean

MONTANA STATE UNIVERSITY  
Bozeman, Montana

March, 1974

ACKNOWLEDGMENTS

I wish to express my deep appreciation to my advisor, Professor N. A. Shyne, for his thoughtful guidance and encouragement in this research. Thanks are also due to Professor J. P. Hanton for his useful suggestions and discussions in this research.

My thanks to the department head, Professor P. E. Uhlrich, for his encouragement and financial support throughout my stay at Montana State University.

My thanks to my parents without whose moral support and encouragement throughout all my graduate work I could not have completed this work. Finally, thanks to my wife, Anita, for typing the entire first draft.

## TABLE OF CONTENTS

	<u>Page</u>
VITA . . . . .	ii
ACKNOWLEDGMENTS . . . . .	iii
TABLE OF CONTENTS . . . . .	iv
LIST OF TABLES . . . . .	vii
LIST OF FIGURES . . . . .	viii
LIST OF SYMBOLS . . . . .	xiii
ABSTRACT . . . . .	xvi
Chapter	
1. INTRODUCTION . . . . .	1
HISTORICAL REVIEW . . . . .	1
Anderson's Theory . . . . .	1
Summary of Other Theories . . . . .	7
PROSPECTS OF DEVELOPMENT AND TECHNOLOGICAL APPLICATION . . . . .	9
CONTENTS OF THE THESIS AND ASSUMPTIONS . .	11
2. CLASSIFICATION OF SEMICONDUCTOR HETEROJUNCTIONS . . . . .	16
INTRODUCTION . . . . .	16
CLASSIFICATION . . . . .	17
IMPORTANCE OF CLASSIFICATION . . . . .	27

	<u>Page</u>
3. ANALYSIS OF ELECTRIC FIELD . . . . .	45
GENERAL THEORY . . . . .	45
BUILT-IN VOLTAGES . . . . .	52
DISTRIBUTION OF CARRIERS . . . . .	60
PRACTICAL MODEL OF n-p SEMICONDUCTOR	
HETEROJUNCTION . . . . .	64
Model and Assumption . . . . .	66
Calculation of Electric Field and	
Capacitance . . . . .	67
4. TEMPERATURE EFFECTS IN SEMICONDUCTOR	
HETEROJUNCTIONS . . . . .	75
TEMPERATURE DEPENDENCE OF CARRIER	
CONCENTRATION . . . . .	76
EVALUATION OF FERMI LEVEL AT DIFFERENT	
TEMPERATURE RANGES . . . . .	79
TEMPERATURE DEPENDENCE OF BUILT-IN	
VOLTAGE . . . . .	83
TEMPERATURE DEPENDENCE OF DISCONTIN-	
UITIES . . . . .	100
5. INTRINSIC SEMICONDUCTOR HETEROJUNCTION . . . . .	105
INTRINSIC CONDUCTIVITY . . . . .	106
THEORY OF INTRINSIC SEMICONDUCTOR	
DEVICES . . . . .	108
DEVICES USING AN INTRINSIC AND AN	
EXTRINSIC SEMICONDUCTOR . . . . .	112
ADVANTAGES OF INTRINSIC SEMICONDUCTOR	
DEVICES . . . . .	113

	<u>Page</u>
6. CONCLUSIONS AND SUGGESTIONS . . . . .	114
APPENDIX	
A. 3-D ENERGY BAND DIAGRAM . . . . .	118
B. CHANGE OF TOTAL ENERGY DISCONTINUITIES ( $\Delta E_C + \Delta E_V$ ) . . . . .	123
BIBLIOGRAPHY . . . . .	128

## LIST OF TABLES

<u>Appendix Table</u>	<u>Page</u>
1. Change in Discontinuities With Changing Temperature for Ge-GaAs Heterojunction . . .	125
2. Change in Discontinuities With Changing Temperature for GaP-Si Heterojunction . . .	126
3. Change in Discontinuities With Changing Temperature for Si-Ge Heterojunction . . .	127

## LIST OF FIGURES

<u>Figure</u>	<u>Page</u>
1. Energy-band diagram for two isolated semiconductors in which space charge neutrality is assumed to exist in every region . . . . .	3
2. Energy-band diagram of a n-p hetero-junction in thermal equilibrium . . . . .	5
3. Energy-band diagram for two isolated semiconductors in which space charge neutrality is assumed to exist in every region with $\chi_{2h} > \chi_{1h} > \chi_{1e} > \chi_{2e}$ . . . . .	19
4. Energy-band diagram for two isolated semiconductors in which space charge neutrality is assumed to exist in every region with $\chi_{1h} = \chi_{2h}$ ; $\chi_{2h} > \chi_{1e} > \chi_{2e}$ . . . . .	19
5. Energy-band diagram for two isolated semiconductors in which space charge neutrality is assumed to exist in every region with $\chi_{1h} > \chi_{2h} > \chi_{1e} > \chi_{2e}$ . . . . .	20
6. Energy-band diagram for two isolated semiconductors in which space charge neutrality is assumed to exist in every region with $\chi_{1h} > \chi_{1e}$ ; $\chi_{1e} = \chi_{2h}$ ; $\chi_{2h} > \chi_{2e}$ . . . . .	20
7. Energy-band diagram for two isolated semiconductors in which space charge neutrality is assumed to exist in every region with $\chi_{1e} > \chi_{2h}$ . . . . .	21
8. Energy-band diagram for two isolated semiconductors in which space charge neutrality is assumed to exist in every region with $\chi_{2h} > \chi_{1h} > \chi_{2e}$ ; $\chi_{2e}$ . . . . .	21

<u>Figure</u>	<u>Page</u>
9. Energy-band diagram for two isolated semiconductors in which space charge neutrality is assumed to exist in every region with $\chi_{2h} > \chi_{1h} > \chi_{2e} > \chi_{1e}$ . . . . .	23
10. Energy-band diagram for two isolated semiconductors in which space charge neutrality is assumed to exist in every region with $\chi_{2h} > \chi_{1h} = \chi_{2e} > \chi_{1e}$ . . . . .	23
11. Energy-band diagram for two isolated semiconductors in which space charge neutrality is assumed to exist in every region with $\chi_{2e} > \chi_{1h}$ . . . . .	24
12. Semiconductor heterojunction classification chart . . . . .	26
13. Energy-band diagram of two semiconductors in thermal equilibrium that defines working space $\chi_{2h} > \chi_{1h} > \chi_{1e} > \chi_{2e}$ . . . . .	28
14. Energy-band diagram of two semiconductors in thermal equilibrium that defines the working space $\chi_{1h} = \chi_{2h}; \chi_{2h} > \chi_{1e} > \chi_{2e}$ . . . . .	31
15. Energy-band diagram of two semiconductors in thermal equilibrium that defines the working space $\chi_{1h} > \chi_{2h} > \chi_{1e} > \chi_{2e}$ . . . . .	33
16. Energy-band diagram of two semiconductors in thermal equilibrium that defines the working space $\chi_{1h} > \chi_{2h}; \chi_{2h} = \chi_{1e}; \chi_{1e} > \chi_{2e}$ . . . . .	35
17. Energy-band diagram of two semiconductors in thermal equilibrium that defines the working space $\chi_{1h} > \chi_{1e} > \chi_{2h} > \chi_{1e}$ . . . . .	35

<u>Figure</u>	<u>Page</u>
18. Energy-band diagram of two semiconductors in thermal equilibrium that defines the working space $\chi_{2h} > \chi_{1h} > \chi_{2e}; \chi_{2e} = \chi_{1e}$ . . . . .	38
19. Energy-band diagram of two semiconductors in thermal equilibrium that defines the working space $\chi_{2h} > \chi_{1h} > \chi_{2e} > \chi_{1e}$ . . . . .	40
20. Energy-band diagram of two semiconductors in thermal equilibrium that defines the working space $\chi_{2h} > \chi_{1h}; \chi_{1h} = \chi_{2e}; \chi_{2e} > \chi_{1e}$ . . . . .	42
21. Energy-band diagram of two semiconductors in thermal equilibrium that defines the working space $\chi_{2h} > \chi_{1h}$ . . . . .	42
22. Energy-band diagram of isolated n-p semiconductors of the same element in which space charge neutrality is assumed to exist in every region . . . . .	49
23. Energy-band diagram of n-p homojunction in thermal equilibrium . . . . .	50
24. Energy-band diagram of two isolated semiconductors in which space charge neutrality is assumed to exist in every region with $\phi_{m_1} < \phi_{m_2}$ . . . . .	54
25. Approximate distribution of carriers near the boundary plane of a germanium p-n junction at room temperature . . . . .	61
26. The approximate distribution of carriers near the boundary plane of an abrupt n-p Ge-GaAs heterojunction in equilibrium at 300°K . . . . .	65

<u>Figure</u>	<u>Page</u>
27. Energy-band diagram of two isolated semiconductors. The n-type impurity has diffused into p-type broad-gap semiconductor, thus forming an n-n heterojunction and an n-p homojunction . . .	68
28. Practical model of semiconductor heterojunction (n-p) in thermal equilibrium . . .	68
29. n-p heterojunction in practice consists of an isotype heterojunction (n-n) and homojunction (n-p). Isotype heterojunction is shown to have shifted "t" units into an n-type semiconductor . . . . .	69
30. Variation of Fermi level with temperature for (a) n-type and (b) p-type semiconductors, of various impurity densities, those marked "2" to intermediate densities, and those marked "3" to relatively high impurity densities . . . . .	84
31. Two isolated semiconductors as discussed in Case 1, space charge neutrality is assumed to exist in every region. (a) at room temperature, (b) at an elevated temperature where narrow-gap semiconductor becomes intrinsic, making built-in-voltage to increase and (c) at a temperature where broad-gap semiconductor also become intrinsic, shows a change in polarity of built-in-voltage if compared with Figure (a) . . . . .	87
32. An approximate plot of built-in voltage at the heterojunction with respect to temperature in Case 1 . . . . .	89
33. Energy-band diagram of isolated Ge-Si in which space charge neutrality is assumed to exist in every region at 300°K . . . . .	90

<u>Figure</u>	<u>Page</u>
34. Energy-band diagram of isolated Ge-Si in which space charge neutrality is assumed to exist in every region at 450°K. . . . .	94
35. Energy-band diagram of isolated Ge-Si in which space charge neutrality is assumed to exist in every region at 600°K . . . . .	96
36. Built-in voltage at the Ge-Si heterojunction as considered in the example of Case 1 . . . .	97
37. Two isolated semiconductors as discussed in Case 2, space charge neutrality is assumed to exist in every region with $\Delta E_v > \Delta E_c$ . (a) At room temperature, (b) at an elevated temperature where narrow-gap semiconductor becomes intrinsic making built-in voltage to change sign, and (c) at a temperature where broad-gap semiconductor also becomes intrinsic, changing the sign of built-in voltage once over again . . . . .	99
38. Built-in voltage at the n-n heterojunction with respect to temperature in Case 2 . . . .	101
39. Change in total discontinuities with changing temperature are plotted for GaP-Si, Ge-GaAs and Ge-Si heterojunctions . . . . .	103
40. Carrier concentration has been plotted for an abrupt intrinsic semiconductor heterojunction, $n_1=p_1 \neq n_2=p_2$ . . . . .	109
41. Energy-band diagram of InAs ± GaSb, in which space charge neutrality is assumed to exist in every region at 300°K . . . . .	111

#### Appendix

B. E - X - K plot of two isolated direct gap semiconductors . . . . .	122
---	-----

## LIST OF SYMBOLS

Subscript "1" represents narrow-gap semiconductor

Subscript "2" represents broad-gap semiconductor

$C$	Capacitance in Farad.
$E_c$	Energy of conduction band gap in eV.
$\Delta E_c$	Energy discontinuity in energy band diagram of a heterojunction (associated with electron affinity difference) in eV.
$E_F$	Fermi level, n and p semiconductor in eV.
$E_{Fi}, E_{FI}$	Intrinsic Fermi level in semiconductor in eV.
$E_g$	Energy band gap in eV.
$E_v$	Energy of valence-band edge in eV.
$\Delta E_v$	Energy discontinuity in the valence-band energy diagram of a heterojunction in eV.
$h$	Planck's constant in Joule-sec.
$\hbar$	$\frac{h}{2\pi}$
$J_n$	Electron current density in $A\text{ cm}^{-2}$ .
$J_p$	Hole current density in $A\text{ cm}^{-2}$ .
$K$	Momentum wave vector.
$k$	Boltzmann's constant in $eV^\circ\text{ k}^{-1}$ .
$m_e^*$	Electron effective mass Kg.
$m_{de}^*$	Density-of-state effective mass for electron in Kg.

$m_{dh}^*$	Density-of-state effective mass for holes in Kg.
$m_{lh}^*$	Light hole mass in Kg.
$m_{hh}^*$	Heavy hole mass in Kg.
$m_l^*$	Effective mass along the longitudinal ellipsoidal energy surface in Kg.
$m_t^*$	Effective mass along the transverse ellipsoidal energy surface in Kg.
$m_h^*$	Effective mass of hole.
$N_a, N_A$	Acceptor density in $\text{cm}^{-3}$ .
$N_C$	Effective density of energy states at the conduction band edge in $\text{cm}^{-3}$ .
$N_d, N_D$	Donor density in $\text{cm}^{-3}$ .
$N_V$	Effective density of energy states at the valence-band edge in $\text{cm}^{-3}$ .
$n_o, n$	Free electron density in the conduction band in $\text{cm}^{-3}$ .
$n_d$	Unionized donors in $\text{cm}^{-3}$ .
$n_i$	Intrinsic carrier concentration in a semiconductor $\text{cm}^{-3}$ .
$p_o, p$	Hole density in $\text{cm}^{-3}$ .
$P_a$	Unionized acceptors in $\text{cm}^{-3}$ .
$q$	Charge of an electron, $1.6 \times 10^{-19}$ coulomb.
$T$	Absolute temperature in $^{\circ}\text{K}$ .
$V_{\text{BHT}}$	Built-in voltage in heterojunction in volts.

$V_{\text{BHM}}$	Built-in voltage in homojunction in volts.
$x$	Distance in cm.
$\gamma$	Emitter injection efficiency.
$\epsilon$	Dielectric constant of the semiconductor in $\text{F cm}^{-1}$ .
$\mu_n$	Mobility of electrons in $\text{cm}^2 \text{v}^{-1} \text{sec}^{-1}$ .
$\mu_p$	Mobility of holes in $\text{cm}^2 \text{v}^{-1} \text{sec}^{-1}$ .
$\phi_m$	Work function of a semiconductor in eV.
$\chi_e$	Electron affinity of a semiconductor in eV.
$\chi_h$	$(\chi_e + E_g)$ in eV.
$\psi(x)$	Electrostatic potential difference as a function of distance in volts.
$\sigma$	Conductivity in mhos.
$\theta$	Debye temperature.

## ABSTRACT

A new classification for semiconductor heterojunctions has been formulated by considering the different mutual positions of conduction-band and valence-band edges. To the nine different classes of semiconductor heterojunction thus obtained, effects of different work functions, different effective masses of carriers and types of semiconductors are incorporated in the classification. General expressions for the built-in voltages in thermal equilibrium have been obtained considering only nondegenerate semiconductors. Built-in voltage at the heterojunction is analyzed. The approximate distribution of carriers near the boundary plane of an abrupt n-p heterojunction in equilibrium is plotted. In the case of a p-n heterojunction; considering diffusion of impurities from one semiconductor to the other, a practical model is proposed and analyzed. The effect of temperature on built-in voltage leads to the conclusion that built-in voltage in a heterojunction can change its sign, in some cases twice, with the choice of an appropriate doping level. The total change of energy discontinuities ( $\Delta E_C + \Delta E_V$ ) with increasing temperature has been studied, and it is found that this change depends on an empirical constant and the 0°K Debye temperature of the two semiconductors. The total change of energy discontinuity can increase or decrease with the temperature. Intrinsic semiconductor-heterojunction devices are studied; band gaps of value less than 0.7 eV. are suggested if such devices are to be used at room temperature. Built-in voltage in the case of intrinsic semiconductor heterojunction devices varies slightly with the temperature. With proper choice of effective masses, the built-in voltage remains essentially constant with the temperature. The advantages of intrinsic semiconductor devices are discussed. A three-dimensional energy-distance-momentum diagram is described; it suggests a change in the wave vector of a carrier, in transit from one semiconductor to other. Thus, the probability of transition of a carrier across the heterojunction is reduced.

## Chapter 1

### INTRODUCTION

#### Historical Review

A semiconductor heterojunction is a junction between two dissimilar semiconductors where the crystal structure is continuous across the interface. Semiconductor heterojunction research is an important area of device study which has evolved from the research of the last decade. The barriers introduced into the energy-band diagram by the energy-gap difference of two semiconductors allows a new degree of freedom to the device designer. For example, in GaAs injection lasers [1], the addition of  $\text{Al}_x\text{Ga}_{1-x}\text{As}$  confinement barriers has resulted in a major reduction in 300°K threshold current densities. Electrooptical effects in heterojunctions that are promising include infrared to visible upconversion systems [2], the window effect [3], solar cells [4] and photo transistors [5]. High yield photo cathodes [6], cold cathodes [7] and electron multipliers [8] of the negative-electron affinity type represent yet other families of devices where heterojunctions are involved.

The heterojunction structure was first considered by Preston [9]. Gubanov [10] produced an analysis of

heterojunctions with n-n, p-p and p-n combinations. Shockley [11] proposed a circuit device incorporating a change in the magnitude of the forbidden gap in the transition region of p-n junction. Kroemer [12] proposed the use of a heterojunction as a wide-gap emitter to increase the injection efficiency of transistors. The Anderson theory [3] is discussed in the following section and a brief summary of other theories is discussed on page 7.

Anderson's Theory. The energy-band model of an ideal abrupt heterojunction without interface states was proposed by Anderson based on the previous work of Shockley. This model is important as it can adequately explain most of the transport processes, and only a slight modification [13] of the model is needed to account for non-ideal cases such as interface states. Consider the energy-band profile of the two isolated semiconductors as shown in Figure 1. The two semiconductors are assumed to have different band gaps ( $E_{g_1}, E_{g_2}$ ), different dielectric constants ( $\epsilon_1, \epsilon_2$ ), different work function ( $\phi_{m_1}, \phi_{m_2}$ ), and different electron affinities ( $\chi_{1e}, \chi_{2e}$ ). The work function is defined as the energy required to remove an electron from the Fermi level ( $E_F$ ) to a position just outside of

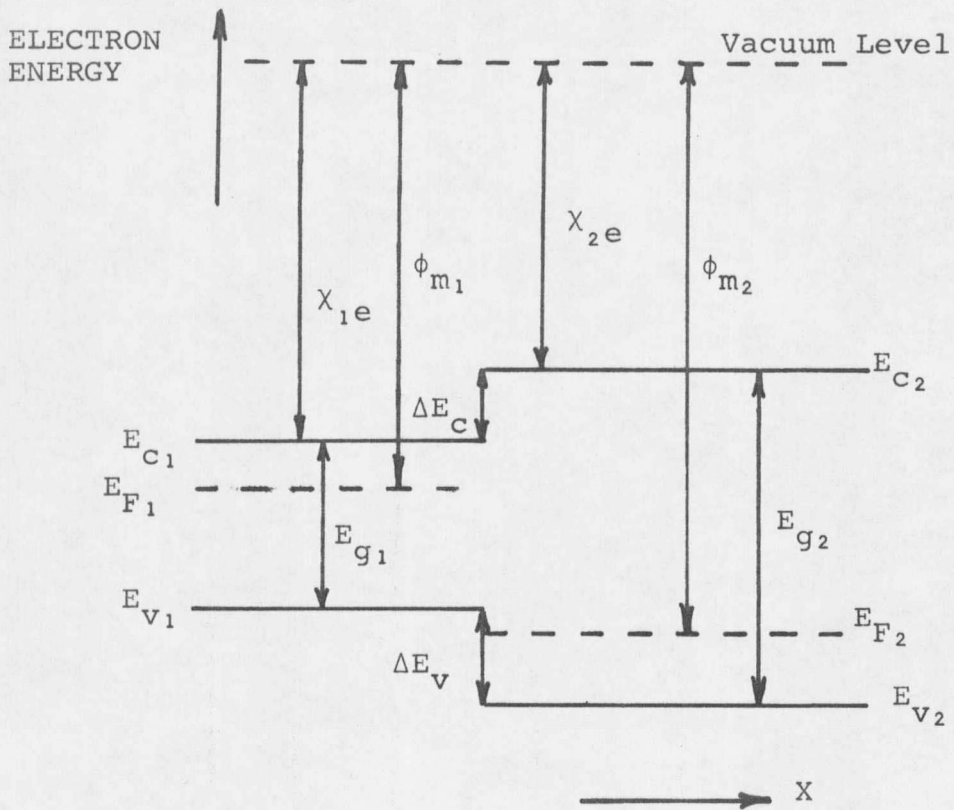


Figure 1. Energy-band diagram for two isolated semiconductors in which space charge neutrality is assumed to exist in every region.

the material. The bottom of the conduction-band is represented by  $E_C$  and the top of the valence-band is represented by  $E_V$ . The subscripts 1 and 2 refer to the narrow-gap and wide-gap semiconductors, respectively. Electron affinity is defined as the energy required to remove an electron from the bottom of conduction-band to a position just outside of the material. It is assumed that space charge neutrality exists in every region and thus band edges ( $E_{C_1}, E_{C_2}, E_{V_1}, E_{V_2}$ ) are shown to be horizontal. The difference in energy of the conduction-band edges in the two materials is represented by  $\Delta E_C$  and that in the valence-band edges is  $\Delta E_V$ .

A junction formed between an n-type narrow-gap semiconductor and a p-type wide-gap semiconductor is considered. The energy-band profile of such a junction at equilibrium is shown in Figure 2.

The electrostatic potential difference between any two points can be represented by the vertical displacement of the band edges between these two points in a semiconductor. An electrostatic field can be represented by the slope of the edges on a band diagram. The total built-in voltage ( $V_{BHT}$ ) is equal to the sum of the partial built-in

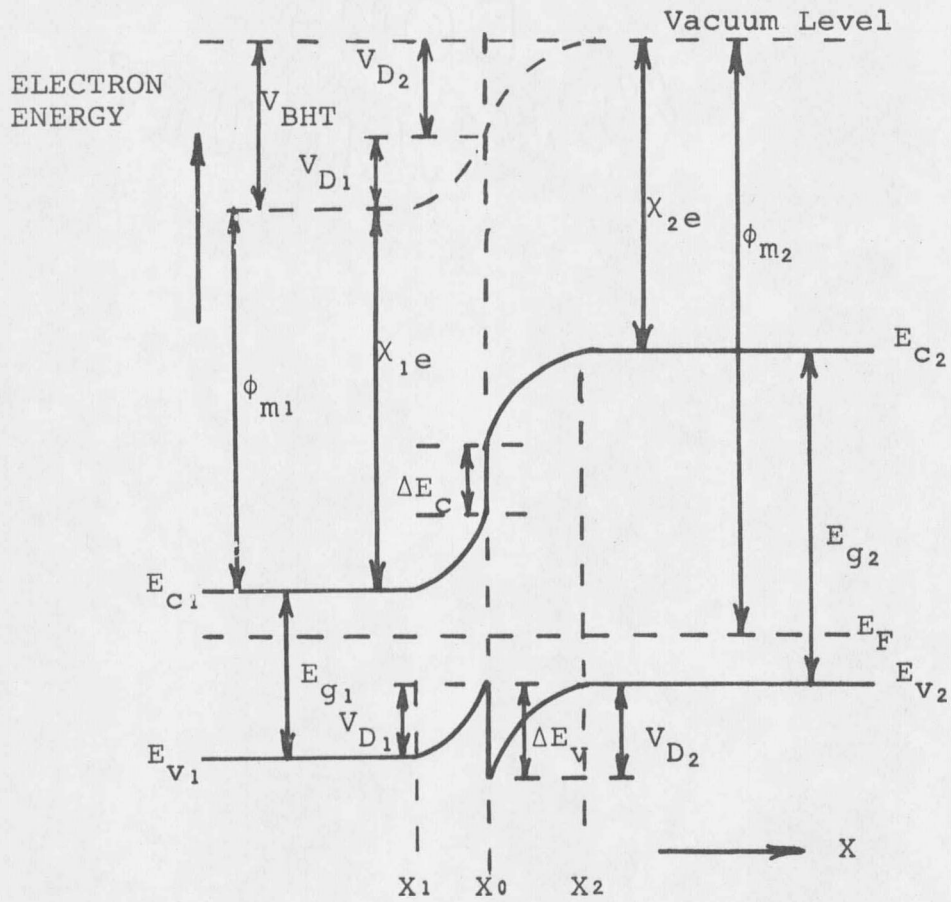


Figure 2. Energy-band diagram of n-p heterojunction in thermal equilibrium.

voltages ( $V_{D_1} + V_{D_2}$ ), where  $V_{D_1}$  and  $V_{D_2}$  are the electrostatic potentials supported at equilibrium by semiconductors 1 and 2, respectively. Since the Fermi level must coincide on both sides in equilibrium and the vacuum level is everywhere parallel to the band edges and is continuous, the discontinuity in the conduction band edges ( $\Delta E_c$ ) and valence-band edges ( $\Delta E_v$ ) is invariant with doping in those cases where  $E_g$  and  $\chi$  are not functions of doping (i.e., nondegenerate semiconductors). A degenerate semiconductor is one in which Fermi level lies in the conduction or in the valence-band. It is assumed that the electron density is zero for  $X > X_1$ , and the hole density is zero for  $X < X_2$ . Then at any point in the transition region, the space charge density is merely equal to the donor or acceptor density.

$$p_1 = q N_{D_1} \quad X_1 < X < X_0$$

$$p_2 = q N_{A_2} \quad X_0 < X < X_2$$

where  $N_{D_1}$  is the donor concentration in semiconductor 1 and  $N_{A_2}$  is the acceptor concentration in semiconductor 2. The solution of Poisson's equation in the one dimensional case with appropriate doping levels gives the solution for an abrupt junction as follows [3]:































































































































































































































































